SIMULATION OF ERGODIC MULTIVARIATE STOCHASTIC PROCESSES

By George Deodatis,[1] Associate Member, ASCE

ABSTRACT: A simulation algorithm is proposed to generate sample functions of a stationary, multivariate stochastic process according to its prescribed cross-spectral density matrix. If the components of the vector process correspond to different locations in space, then the process is nonhomogeneous in space. The ensemble cross-correlation matrix of the generated sample functions is identical to the corresponding target. The simulation algorithm generates ergodic sample functions in the sense that the temporal cross-correlation matrix of each and every generated sample function is identical to the corresponding target, when the length of the generated sample function is equal to one period (the generated sample functions are periodic). The proposed algorithm is based on an extension of the spectral representation method and is very efficient computationally since it takes advantage of the fast Fourier transform technique. The generated sample functions are Gaussian in the limit as the number of terms in the frequency discretization of the cross-spectral density matrix approaches infinity. An example involving simulation of turbulent wind velocity fluctuations is presented in order to demonstrate the capabilities and efficiency of the proposed algorithm.

INTRODUCTION

Several methods are currently available to solve a large number of problems in mechanics involving uncertain quantities described by stochastic processes, fields, or waves. At this time, however, Monte Carlo simulation appears to be the only universal method that can provide accurate solutions for certain problems in stochastic mechanics involving nonlinearity, system stochasticity, stochastic stability, parametric excitations, large variations of uncertain parameters, etc., and that can assess the accuracy of other approximate methods such as perturbation, statistical linearization, closure techniques, stochastic averaging, etc.

One of the most important parts of the Monte Carlo-simulation methodology is the generation of sample functions of the stochastic processes, fields, or waves involved in the problem. The generated sample functions must accurately describe the probabilistic characteristics of the corresponding stochastic processes, fields, or waves that may be either stationary or nonstationary, homogeneous or nonhomogeneous, one-dimensional or multidimensional, univariate or multivariate, and Gaussian or non-Gaussian. Among the various methods that have been developed to generate such sample functions [for a review of these methods, the reader is referred to Elishakoff (1983), Kozin (1988), Soong and Grigoriu (1993), Grigoriu (1995), Deodatis (1996)], the spectral representation method is one of the most widely used today. Although the concept of the method existed for some time (Rice 1954), it was Shinozuka (Shinozuka and Jan 1972; Shinozuka 1972) who first applied it for simulation purposes including multidimensional, multivariate, and nonstationary cases. Yang (1972, 1973) showed that the fast Fourier transform (FFT) technique can be used to dramatically improve the computational efficiency of the spectral representation algorithm, and proposed a formula to simulate random envelope processes. Shinozuka (1974) extended the application of the FFT technique to multidimensional cases. Deodatis and Shinozuka (1989) further extended the spectral representation method to simulate stochastic waves, Yamazaki and Shinozuka (1988) developed an iterative procedure to simulate non-Gaussian stochastic fields, and Grigoriu (1993) compared two different spectral representation models. Three review papers on the subject of simulation using the spectral representation method were written by Shinozuka (1987) and Shinozuka and Deodatis (1988, 1991).

This paper introduces an extension of the spectral representation method to simulate ergodic stochastic vector processes. Although an algorithm based on the spectral representation method was available from the early seventies to simulate multivariate stochastic processes (Shinozuka and Jan 1972), this algorithm was generating sample functions that were not ergodic. Several attempts have been made to modify the Shinozuka and Jan (1972) algorithm in order to achieve ergodicity. In one of the latest of these attempts, Shinozuka et al. (1989) introduced the idea of double-indexing the frequencies, but the formula suggested in that paper was still generating sample functions that were not ergodic.

The spectral-representation-based algorithm proposed in this paper succeeds in generating ergodic sample functions of a stochastic vector process, using the idea of double-indexing the frequencies. The proposed algorithm is simple and straightforward, generates sample functions of the vector process according to a prescribed target cross-spectral density matrix, and is very efficient computationally since it is taking advantage of the fast Fourier transform technique.

At this juncture, it should be pointed out that if the components of the vector process correspond to different locations in space, then the process is nonhomogeneous in space (this is the case in the wind velocity fluctuations example provided at the end of this paper).

Finally, from the rich bibliography related to the various methods currently available to generate sample functions of stochastic processes, fields, and waves, the following representative publications dealing with the simulation of multivariate stochastic processes are mentioned here: Gersch and Yonemoto (1977) [multivariate autoregressive moving average (ARMA) model], Mignolet and Spanos (1987) (stability and invertibility aspects of autoregressive (AR) to ARMA procedures for multivariate random processes), Kareem and Li (1991) (simulation of nonstationary vector processes using an FFT-based approach), Li and Kareem (1993) (simulation of multivariate processes using a hybrid discrete Fourier transform and digital filtering approach), Ramadan and Novak (1993) (asymptotic and approximate spectral techniques to simulate multidimensional and multivariate processes and fields).

In the remaining part of this paper, the theory and the simulation algorithm are presented for trivariate stochastic vector processes (dimension of vector process is three). This is done for the sake of simplicity in the notation. The proposed algorithm can be extended in a straightforward fashion to any other dimension of the vector process.

[1]Asst. Prof., Dept. of Civ. Engrg. and Operations Res., Princeton Univ., Princeton, NJ 08544.

Note. Associate Editor: Mircea D. Grigoriu. Discussion open until January 1, 1997. To extend the closing date one month, a written request must be filed with the ASCE Manager of Journals. The manuscript for this paper was submitted for review and possible publication on July 28, 1994. This paper is part of the ***Journal of Engineering Mechanics***, Vol. 122, No. 8, August, 1996. ©ASCE, ISSN 0733-9399/96/0008-0778–0787/$4.00 + $.50 per page. Paper No. 8943.

J. Eng. Mech. 1996.122:778-787.

TRIVARIATE STATIONARY STOCHASTIC VECTOR PROCESSES

Consider a one-dimensional, trivariate (1D-3V) stationary stochastic vector process with components $f_1^0(t)$, $f_2^0(t)$, and $f_3^0(t)$, having mean value equal to zero

$$\varepsilon[f_j^0(t)] = 0; j = 1, 2, 3 \tag{1}$$

the cross-correlation matrix is given by

$$\mathbf{R}^0(\tau) = \begin{bmatrix} R_{11}^0(\tau) & R_{12}^0(\tau) & R_{13}^0(\tau) \\ R_{21}^0(\tau) & R_{22}^0(\tau) & R_{23}^0(\tau) \\ R_{31}^0(\tau) & R_{32}^0(\tau) & R_{33}^0(\tau) \end{bmatrix} \tag{2}$$

and the cross-spectral density matrix is given by

$$\mathbf{S}^0(\omega) = \begin{bmatrix} S_{11}^0(\omega) & S_{12}^0(\omega) & S_{13}^0(\omega) \\ S_{21}^0(\omega) & S_{22}^0(\omega) & S_{23}^0(\omega) \\ S_{31}^0(\omega) & S_{32}^0(\omega) & S_{33}^0(\omega) \end{bmatrix} \tag{3}$$

In (2), $R_{jj}^0(\tau)$; $j = 1, 2, 3$ = autocorrelation functions of the three components $f_j^0(t)$; $j = 1, 2, 3$ of the process and $R_{jk}^0(\tau)$, $j = 1, 2, 3$, $k = 1, 2, 3$, $j \neq k$ = the corresponding cross-correlation functions. Due to the stationarity hypothesis, the following relations are valid:

$$R_{jj}^0(\tau) = R_{jj}^0(-\tau), j = 1, 2, 3 \tag{4}$$

$$R_{jk}^0(\tau) = R_{kj}^0(-\tau), j = 1, 2, 3; k = 1, 2, 3; j \neq k \tag{5}$$

The elements of the cross-correlation matrix are related to the corresponding elements of the cross-spectral density matrix through the Wiener-Khintchine transformation (τ is the time lag and ω is the frequency)

$$S_{jk}^0(\omega) = \frac{1}{2\pi} \int_{-\infty}^{\infty} R_{jk}^0(\tau) e^{-i\omega\tau}\, d\tau, j, k = 1, 2, 3 \tag{6}$$

$$R_{jk}^0(\tau) = \int_{-\infty}^{\infty} S_{jk}^0(\omega) e^{i\omega\tau}\, d\omega, j, k = 1, 2, 3 \tag{7}$$

In (3), $S_{jj}^0(\omega)$, $j = 1, 2, 3$ = power spectral density functions of the three components of the process; and $S_{jk}^0(\omega)$, $j = 1, 2, 3$, $k = 1, 2, 3$, $j \neq k$ = corresponding cross-spectral density functions. While the power spectral density function is a real and nonnegative function of ω, the cross-spectral density function is a generally complex function of ω. Because of (4)–(7), the following relations are valid:

$$S_{jj}^0(\omega) = S_{jj}^0(-\omega), j = 1, 2, 3 \tag{8}$$

$$S_{jk}^0(\omega) = S_{jk}^{0*}(-\omega), j = 1, 2, 3; k = 1, 2, 3; j \neq k \tag{9}$$

$$S_{jk}^0(\omega) = S_{kj}^{0*}(\omega), j = 1, 2, 3; k = 1, 2, 3; j \neq k \tag{10}$$

where the asterisk denotes the complex conjugate. Eq. (10) indicates that the cross-spectral density matrix $\mathbf{S}^0(\omega)$ is Hermitian. It can also be shown (Shinozuka 1987) that matrix $\mathbf{S}^0(\omega)$ is nonnegative definite.

SIMULATION FORMULA

In the following, distinction will be made between the stochastic vector process $f_j^0(t)$, $j = 1, 2, 3$ and its simulation $f_j(t)$, $j = 1, 2, 3$.

To simulate the 1D-3V stationary stochastic process $f_j^0(t)$, $j = 1, 2, 3$, its cross-spectral density matrix $\mathbf{S}^0(\omega)$ must be first decomposed into the following product:

$$\mathbf{S}^0(\omega) = \mathbf{H}(\omega)\mathbf{H}^{T*}(\omega) \tag{11}$$

where superscript ^{T} = transpose of a matrix. This decomposition can be performed using Cholesky's method, in which case $\mathbf{H}(\omega)$ is a lower triangular matrix

$$\mathbf{H}(\omega) = \begin{bmatrix} H_{11}(\omega) & 0 & 0 \\ H_{21}(\omega) & H_{22}(\omega) & 0 \\ H_{31}(\omega) & H_{32}(\omega) & H_{33}(\omega) \end{bmatrix} \tag{12}$$

whose diagonal elements are real and nonnegative functions of ω, and whose off-diagonal elements are generally complex functions of ω. The following relations are valid for the elements of matrix $\mathbf{H}(\omega)$:

$$H_{jj}(\omega) = H_{jj}(-\omega), j = 1, 2, 3 \tag{13}$$

$$H_{jk}(\omega) = H_{jk}^*(-\omega), j = 2, 3; k = 1, 2; j > k \tag{14}$$

If the off-diagonal elements $H_{jk}(\omega)$ are written in polar form as

$$H_{jk}(\omega) = |H_{jk}(\omega)| e^{i\theta_{jk}(\omega)}, j = 2, 3; k = 1, 2; j > k \tag{15}$$

where

$$\theta_{jk}(\omega) = \tan^{-1}\left\{\frac{\text{Im}[H_{jk}(\omega)]}{\text{Re}[H_{jk}(\omega)]}\right\} \tag{16}$$

with Im and Re = imaginary and real parts, respectively, of a complex number, then (14) is written equivalently as

$$|H_{jk}(\omega)| = |H_{jk}(-\omega)|, j = 2, 3; k = 1, 2; j > k \tag{17}$$

$$\theta_{jk}(\omega) = -\theta_{jk}(-\omega), j = 2, 3; k = 1, 2; j > k \tag{18}$$

Once matrix $\mathbf{S}^0(\omega)$ is decomposed according to (11)–(12), the stochastic process $f_j^0(t)$, $j = 1, 2, 3$ can be simulated by the following series as $N \to \infty$

$$f_j(t) = 2 \sum_{m=1}^{3} \sum_{l=1}^{N} |H_{jm}(\omega_{ml})| \sqrt{\Delta\omega} \cos[\omega_{ml} t - \theta_{jm}(\omega_{ml}) + \Phi_{ml}],$$

$$j = 1, 2, 3 \tag{19}$$

or explicitly

$$f_1(t) = 2 \sum_{l=1}^{N} |H_{11}(\omega_{1l})| \sqrt{\Delta\omega} \cos[\omega_{1l} t - \theta_{11}(\omega_{1l}) + \Phi_{1l}] \tag{20a}$$

$$f_2(t) = 2 \sum_{l=1}^{N} |H_{21}(\omega_{1l})| \sqrt{\Delta\omega} \cos[\omega_{1l} t - \theta_{21}(\omega_{1l}) + \Phi_{1l}]$$

$$+ 2 \sum_{l=1}^{N} |H_{22}(\omega_{2l})| \sqrt{\Delta\omega} \cos[\omega_{2l} t - \theta_{22}(\omega_{2l}) + \Phi_{2l}] \tag{20b}$$

$$f_3(t) = 2 \sum_{l=1}^{N} |H_{31}(\omega_{1l})| \sqrt{\Delta\omega} \cos[\omega_{1l} t - \theta_{31}(\omega_{1l}) + \Phi_{1l}]$$

$$+ 2 \sum_{l=1}^{N} |H_{32}(\omega_{2l})| \sqrt{\Delta\omega} \cos[\omega_{2l} t - \theta_{32}(\omega_{2l}) + \Phi_{2l}]$$

$$+ 2 \sum_{l=1}^{N} |H_{33}(\omega_{3l})| \sqrt{\Delta\omega} \cos[\omega_{3l} t - \theta_{33}(\omega_{3l}) + \Phi_{3l}] \tag{20c}$$

where the double-indexing of the frequencies (Shinozuka et al. 1989) is defined as:

$$\omega_{1l} = l\Delta\omega - \frac{2}{3}\Delta\omega, l = 1, 2, \ldots, N \tag{21a}$$

$$\omega_{2l} = l\Delta\omega - \frac{1}{3}\Delta\omega, l = 1, 2, \ldots, N \tag{21b}$$

$$\omega_{3l} = l\Delta\omega, l = 1, 2, \ldots, N \tag{21c}$$

$$\Delta\omega = \frac{\omega_u}{N} \tag{22}$$

$$\theta_{jm}(\omega_{ml}) = \tan^{-1}\left\{\frac{\mathrm{Im}[H_{jm}(\omega_{ml})]}{\mathrm{Re}[H_{jm}(\omega_{ml})]}\right\} \tag{23}$$

In (22), ω_u = an upper cutoff frequency beyond which the elements of the cross-spectral density matrix [(3)] may be assumed to be zero for either mathematical or physical reasons. As such, ω_u is a fixed value and hence $\Delta\omega \to 0$ as $N \to \infty$ so that $N\Delta\omega = \omega_u$. A criterion to estimate the value of ω_u can be found in Shinozuka and Deodatis (1991).

The Φ_{1l}, Φ_{2l}, Φ_{3l}, $l = 1, 2, \ldots, N$ appearing in (19)–(20) are three sequences of independent random phase angles distributed uniformly over the interval $[0, 2\pi]$.

It is a straightforward task to show that the following three summations:

$$\sum_{l=1}^{N} A_{1l}\cos[\omega_{1l}t + \rho_{1l}]; \quad \sum_{l=1}^{N} A_{2l}\cos[\omega_{2l}t + \rho_{2l}];$$

$$\sum_{l=1}^{N} A_{3l}\cos[\omega_{3l}t + \rho_{3l}] \tag{24a–c}$$

where the A and ρ = amplitudes and phase angles, respectively, are periodic with respective periods

$$3\frac{2\pi}{\Delta\omega}, 3\frac{2\pi}{\Delta\omega}, \frac{2\pi}{\Delta\omega} \tag{25}$$

Following (24)–(25), the simulated stochastic process $f_j(t)$, $j = 1, 2, 3$ is periodic, with period T_0 given by

$$T_0 = 3\frac{2\pi}{\Delta\omega} \tag{26}$$

Eq. (26) indicates that the smaller the $\Delta\omega$, or equivalently the larger the N under a specified upper cutoff frequency ω_u, the longer the period of the simulated stochastic process.

Another very important point is that the simulated stochastic process $f_j(t)$, $j = 1, 2, 3$ is asymptotically Gaussian as $N \to \infty$ because of the central limit theorem (Shinozuka and Deodatis 1991).

A sample function $f_j^{(i)}(t)$, $j = 1, 2, 3$ of the simulated stochastic process $f_j(t)$, $j = 1, 2, 3$ can be obtained by replacing the three sequences of random phase angles Φ_{1l}, Φ_{2l}, Φ_{3l}, $l = 1, 2, \ldots, N$ with their respective ith realizations $\phi_{1l}^{(i)}$, $\phi_{2l}^{(i)}$, $\phi_{3l}^{(i)}$, $l = 1, 2, \ldots, N$

$$f_j^{(i)}(t) = 2\sum_{m=1}^{3}\sum_{l=1}^{N}|H_{jm}(\omega_{ml})|\sqrt{\Delta\omega}\cos[\omega_{ml}t - \theta_{jm}(\omega_{ml}) + \phi_{ml}^{(i)}],$$

$$j = 1, 2, 3 \tag{27}$$

At this point it should be noted that when generating sample functions of the simulated stochastic process according to (27), the time step Δt separating the generated values of $f_j^{(i)}(t)$ in the time domain has to obey the condition

$$\Delta t \le \frac{2\pi}{2\omega_u} \tag{28}$$

The condition set on Δt in (28) is necessary in order to avoid aliasing according to the sampling theorem [e.g., Bracewell (1986)].

Another interesting point is that the generated values of $f_j^{(i)}(t)$ according to (27) are bounded as follows:

$$f_j^{(i)}(t) \le 2\sum_{m=1}^{3}\sum_{l=1}^{N}|H_{jm}(\omega_{ml})|\sqrt{\Delta\omega}, j = 1, 2, 3 \tag{29}$$

In a subsequent section on numerical examples, it will be demonstrated that for a specific form of the cross-spectral density matrix, the foregoing bound is large enough for all practical applications, even for relatively small values of N. It is obvious that this bound can be easily calculated for any form of the cross-spectral density matrix to be used.

It will be shown now that the ensemble expected value $\varepsilon[f_j(t)]$, $j = 1, 2, 3$ and the ensemble auto-/cross-correlation function $R_{jk}(\tau)$, $j, k = 1, 2, 3$ of the simulated stochastic process $f_j(t)$ are identical to the corresponding targets, $\varepsilon[f_j^0(t)] = 0$, $j = 1, 2, 3$ and $R_{jk}^0(\tau)$, $j, k = 1, 2, 3$, respectively.

1. Show that: $\varepsilon[f_j(t)] = \varepsilon[f_j^0(t)] = 0$, $j = 1, 2, 3$

   Proof: This proof is trivial and similar to the corresponding one for 1D-1V processes (Shinozuka and Deodatis 1991).
2. Show that: $R_{jk}(\tau) = R_{jk}^0(\tau)$, $j, k = 1, 2, 3$

   Proof: Utilizing the property that the operations of mathematical expectation and summation are commutative, the ensemble auto-/cross-correlation function of the simulated stochastic process $f_j(t)$, $j = 1, 2, 3$ can be written as

$$R_{jk}(\tau) = \varepsilon[f_j(t)f_k(t+\tau)]$$

$$= 4\sum_{m_1=1}^{3}\sum_{m_2=1}^{3}\sum_{l_1=1}^{N}\sum_{l_2=1}^{N}|H_{jm_1}(\omega_{m_1l_1})||H_{km_2}(\omega_{m_2l_2})|\Delta\omega\cdot\varepsilon\{\cos[\omega_{m_1l_1}t$$

$$- \theta_{jm_1}(\omega_{m_1l_1}) + \Phi_{m_1l_1}]\cdot\cos[\omega_{m_2l_2}(t+\tau) - \theta_{km_2}(\omega_{m_2l_2}) + \Phi_{m_2l_2}]\} \tag{30}$$

Since the Φs are independent random variables distributed uniformly over the interval $[0, 2\pi]$, the expected value appearing in (30) is different from zero only when

$$m_1 = m_2 = m \text{ and } l_1 = l_2 = l \tag{31}$$

Under the conditions of (31), (30) can be written as

$$R_{jk}(\tau) = 4\sum_{m=1}^{3}\sum_{l=1}^{N}|H_{jm}(\omega_{ml})||H_{km}(\omega_{ml})|\Delta\omega\cdot\frac{1}{2}\varepsilon\{\cos[2\omega_{ml}t$$

$$+ \omega_{ml}\tau - \theta_{jm}(\omega_{ml}) - \theta_{km}(\omega_{ml}) + 2\Phi_{ml}]$$

$$+ \cos[\omega_{ml}\tau + \theta_{jm}(\omega_{ml}) - \theta_{km}(\omega_{ml})]\}$$

$$= 2\sum_{m=1}^{3}\sum_{l=1}^{N}|H_{jm}(\omega_{ml})||H_{km}(\omega_{ml})|\Delta\omega\cdot\cos[\omega_{ml}\tau$$

$$+ \theta_{jm}(\omega_{ml}) - \theta_{km}(\omega_{ml})] \tag{32}$$

Taking into account (13), (17), and (18), the expression for $R_{jk}(\tau)$ in (32) can be written in the limit as $\Delta\omega \to 0$ and $N \to \infty$ (while keeping in mind that $\omega_u = N\Delta\omega$ is constant and that the elements of the cross-spectral density matrix $\mathbf{S}^0(\omega)$ are zero for $|\omega| \ge \omega_u$) in the following way:

$$R_{jk}(\tau) = \int_{-\infty}^{\infty}\sum_{m=1}^{3}|H_{jm}(\omega)||H_{km}(\omega)|e^{i[\omega\tau+\theta_{jm}(\omega)-\theta_{km}(\omega)]}\,d\omega \tag{33}$$

Using now the polar form representation of the elements of the $\mathbf{H}(\omega)$ matrix [(15)], (33) is written as

$$R_{jk}(\tau) = \int_{-\infty}^{\infty}\sum_{m=1}^{3}H_{jm}(\omega)H_{km}^{*}(\omega)e^{i\omega\tau}\,d\omega \tag{34}$$

Then, using the decomposition shown in (11), it is straightforward to show that

$$R_{jk}(\tau) = \int_{-\infty}^{\infty}S_{jk}^0(\omega)e^{i\omega\tau}\,d\omega \tag{35}$$

Comparing finally (7) and (35), it is evident that

$$R_{jk}(\tau) = R^0_{jk}(\tau),\ j,\ k = 1,\ 2,\ 3 \tag{36}$$

For information concerning the rate of convergence of the ensemble auto-/cross-correlation function $R_{jk}(\tau)$, j, $k = 1, 2, 3$ to the corresponding target $R^0_{jk}(\tau)$, j, $k = 1, 2, 3$ as $N \to \infty$ [process of obtaining (33) from (32)], the reader is referred to Shinozuka and Deodatis (1991).

ERGODICITY OF SIMULATED STOCHASTIC VECTOR PROCESS

An important property of the simulated stochastic vector process is the following: each and every sample function given by (27) is ergodic in the mean value and in correlation.

It will be shown now that the temporal average and the temporal auto-/cross-correlation function of any sample function $f^{(i)}_j(t)$, $j = 1, 2, 3$ are identical to the corresponding targets, $\varepsilon[f^{(i)}_j(t)] = 0$, $j = 1, 2, 3$ and $R^0_{jk}(\tau)$, j, $k = 1, 2, 3$, respectively. In addition, it will be shown that these two identities are valid only when the length of the sample function $f^{(i)}_j(t)$, $j = 1, 2, 3$ is equal to the period T_0 given by (26).

1. Show that: $\langle f^{(i)}_j(t)\rangle_T = \varepsilon[f^0_j(t)] = 0$, $j = 1, 2, 3$ when $T = T_0$

   Proof: The temporal average $\langle f^{(i)}_j(t)\rangle_T$ of sample function $f^{(i)}_j(t)$, $j = 1, 2, 3$ over a time interval equal to T can be written as

$$\langle f^{(i)}_j(t)\rangle_T = \frac{1}{T}\int_0^T f^{(i)}_j(t)\,dt = \frac{1}{T}\int_0^T \cdot 2\sum_{m=1}^{3}\sum_{l=1}^{N} |H_{jm}(\omega_{ml})|\sqrt{\Delta\omega}\cos[\omega_{ml}t - \theta_{jm}(\omega_{ml}) + \phi^{(i)}_{ml}]\,dt \tag{37}$$

   The integrand in (37) is a periodic function of t with period equal to T_0. It is therefore obvious that

$$\langle f^{(i)}_j(t)\rangle_T = 0 = \varepsilon[f^0_j(t)],\ j = 1, 2, 3 \text{ when } T = T_0 \tag{38}$$

   with T_0 given by (26). The meaning of (38) is that the temporal average of any sample function $f^{(i)}_j(t)$, $j = 1, 2, 3$ is identical to the target mean value when the length of the sample function is equal to the period T_0.

2. Show that: $R^{(i)}_{jk}(\tau) = R^0_{jk}(\tau)$, j, $k = 1, 2, 3$ when $T = T_0$

   Proof: The temporal auto-/cross-correlation function $R^{(i)}_{jk}(\tau)$, j, $k = 1, 2, 3$ of sample function $f^{(i)}_j(t)$, $j = 1, 2, 3$ over a time interval equal to T is written as

$$R^{(i)}_{jk}(\tau) = \langle f^{(i)}_j(t) f^{(i)}_k(t+\tau)\rangle_T = \frac{1}{T}\int_0^T f^{(i)}_j(t) f^{(i)}_k(t+\tau)\,dt$$

$$= \frac{1}{T}\int_0^T 4\sum_{m_1=1}^{3}\sum_{m_2=1}^{3}\sum_{l_1=1}^{N}\sum_{l_2=1}^{N} |H_{jm_1}(\omega_{m_1l_1})||H_{km_2}(\omega_{m_2l_2})|\Delta\omega \cdot\cos[\omega_{m_1l_1}t - \theta_{jm_1}(\omega_{m_1l_1}) + \phi^{(i)}_{m_1l_1}]$$

$$\cdot\cos[\omega_{m_2l_2}(t+\tau) - \theta_{km_2}(\omega_{m_2l_2}) + \phi^{(i)}_{m_2l_2}]\,dt = \frac{2}{T}\sum_{m_1=1}^{3}\sum_{m_2=1}^{3}\sum_{l_1=1}^{N}\sum_{l_2=1}^{N} |H_{jm_1}(\omega_{m_1l_1})||H_{km_2}(\omega_{m_2l_2})|\Delta\omega\cdot\left\{\int_0^T \cos[(\omega_{m_1l_1} + \omega_{m_2l_2})t + \omega_{m_2l_2}\tau - \theta_{jm_1}(\omega_{m_1l_1}) - \theta_{km_2}(\omega_{m_2l_2}) + \phi^{(i)}_{m_1l_1} + \phi^{(i)}_{m_2l_2}]\,dt + \int_0^T \cos[(\omega_{m_2l_2} - \omega_{m_1l_1})t + \omega_{m_2l_2}\tau + \theta_{jm_1}(\omega_{m_1l_1}) - \theta_{km_2}(\omega_{m_2l_2}) + \phi^{(i)}_{m_2l_2} - \phi^{(i)}_{m_1l_1}]\,dt\right\} \tag{39}$$

It is now straightforward to show the validity of the following two identities:

$$\int_0^T \cos[(\omega_{m_1l_1} + \omega_{m_2l_2})t]\,dt$$

$$= 0 \text{ for any combination of } l_1,\ l_2,\ m_1,\ m_2, \text{ when } T = T_0$$

$$= 3\,\frac{2\pi}{\Delta\omega} \tag{40}$$

$$\int_0^T \cos[(\omega_{m_2l_2} - \omega_{m_1l_1})t]\,dt$$

$$= 0 \text{ for any combination of } l_1,\ l_2,\ m_1,\ m_2, \text{ except for the case:}$$

$$l_1 = l_2 \text{ and } m_1 = m_2, \text{ when } T = T_0 = 3\,\frac{2\pi}{\Delta\omega} \tag{41}$$

Making use of the two identities shown in (40) and (41), the temporal auto-/cross-correlation function $R^{(i)}_{jk}(\tau)$, j, $k = 1, 2, 3$ of sample function $f^{(i)}_j(t)$, $j = 1, 2, 3$ becomes

$$R^{(i)}_{jk}(\tau) = \frac{2}{T_0}\sum_{m=1}^{3}\sum_{l=1}^{N} |H_{jm}(\omega_{ml})||H_{km}(\omega_{ml})|\Delta\omega\cdot\int_0^{T_0} \cdot\cos[\omega_{ml}\tau + \theta_{jm}(\omega_{ml}) - \theta_{km}(\omega_{ml})]\,dt$$

$$= 2\sum_{m=1}^{3}\sum_{l=1}^{N} |H_{jm}(\omega_{ml})||H_{km}(\omega_{ml})|\Delta\omega\cdot\cos[\omega_{ml}\tau + \theta_{jm}(\omega_{ml}) - \theta_{km}(\omega_{ml})] \text{ for } T = T_0 \tag{42}$$

Comparing, finally, (42) with (32), the following conclusion can be drawn:

$$R^{(i)}_{jk}(\tau) = \langle f^{(i)}_j(t) f^{(i)}_k(t+\tau)\rangle_T = R^0_{jk}(\tau),\ j,\ k = 1, 2, 3 \text{ when } T = T_0 \tag{43}$$

It is reminded that (43) is valid in the limit as $\Delta\omega \to 0$ and $N \to \infty$, while keeping in mind that $\omega_u = N\Delta\omega$ is constant and that the elements of the cross-spectral density matrix $\mathbf{S}^0(\omega)$ are zero for $|\omega| \geq \omega_u$. The meaning of (43) is that the temporal auto-/cross-correlation function of any sample function $f^{(i)}_j(t)$, $j = 1, 2, 3$ is identical to the target auto-/cross-correlation function when the length of the sample function is equal to the period T_0.

For information concerning the rate of convergence of the temporal auto-/cross-correlation function $R^{(i)}_{jk}(\tau)$, j, $k = 1, 2, 3$ to the corresponding target $R^0_{jk}(\tau)$, j, $k = 1, 2, 3$ as $N \to \infty$ [process of obtaining (33) from (42)], the reader is referred to Shinozuka and Deodatis (1991).

USE OF FAST FOURIER TRANSFORM TECHNIQUE

The cost of digitally generating sample functions of the simulated stochastic vector process can be drastically reduced by using the FFT technique [e.g., Brigham (1988)]. To take advantage of the FFT technique, (27) is rewritten explicitly in the following form:

$$f^{(i)}_1(p\Delta t) = \text{Re}\left\{h^{(i)}_{11}(p\Delta t)\cdot\exp\left[i\left(\frac{\Delta\omega}{3}\right)(p\Delta t)\right]\right\},$$

$$p = 0, 1, \ldots, 3M - 1 \tag{44a}$$

$$f^{(i)}_2(p\Delta t) = \text{Re}\left\{h^{(i)}_{21}(p\Delta t)\cdot\exp\left[i\left(\frac{\Delta\omega}{3}\right)(p\Delta t)\right]\right\} + \text{Re}\left\{h^{(i)}_{22}(p\Delta t)\cdot\exp\left[i\left(\frac{2\Delta\omega}{3}\right)(p\Delta t)\right]\right\},$$

$$p = 0, 1, \ldots, 3M - 1 \tag{44b}$$

$$f_3^{(i)}(p\Delta t) = \text{Re}\left\{h_{31}^{(i)}(p\Delta t)\cdot\exp\left[i\left(\frac{\Delta\omega}{3}\right)(p\Delta t)\right]\right\} + \text{Re}\left\{h_{32}^{(i)}(p\Delta t)\cdot\exp\left[i\left(\frac{2\Delta\omega}{3}\right)(p\Delta t)\right]\right\} + \text{Re}\left\{h_{33}^{(i)}(p\Delta t)\cdot\exp[i(\Delta\omega)(p\Delta t)]\right\},\ p = 0, 1, \ldots, 3M - 1 \tag{44c}$$

where Re = real part; and $h_{jm}^{(i)}(p\Delta t)$, $j = 1, 2, 3$, $m = 1, 2, 3$, $j \geq m$ stands for

$$h_{jm}^{(i)}(p\Delta t) = \begin{cases} g_{jm}^{(i)}(p\Delta t) & \text{for } p = 0, 1, \ldots, M - 1 \\ g_{jm}^{(i)}[(p - M)\Delta t] & \text{for } p = M, M + 1, \ldots, 2M - 1 \\ g_{jm}^{(i)}[(p - 2M)\Delta t] & \text{for } p = 2M, 2M + 1, \ldots, 3M - 1, \\ & \quad j = 1, 2, 3, m = 1, 2, 3, j \geq m \end{cases} \tag{45}$$

while $g_{jm}^{(i)}(p\Delta t)$, $j = 1, 2, 3$, $m = 1, 2, 3$, $j \geq m$ is defined as

$$g_{11}^{(i)}(p\Delta t) = \sum_{l=0}^{M-1} B_{11l}\cdot\exp[i(l\Delta\omega)(p\Delta t)],\ p = 0, 1, \ldots, M - 1 \tag{46a}$$

$$g_{21}^{(i)}(p\Delta t) = \sum_{l=0}^{M-1} B_{21l}\cdot\exp[i(l\Delta\omega)(p\Delta t)],\ p = 0, 1, \ldots, M - 1 \tag{46b}$$

$$g_{22}^{(i)}(p\Delta t) = \sum_{l=0}^{M-1} B_{22l}\cdot\exp[i(l\Delta\omega)(p\Delta t)],\ p = 0, 1, \ldots, M - 1 \tag{46c}$$

$$g_{31}^{(i)}(p\Delta t) = \sum_{l=0}^{M-1} B_{31l}\cdot\exp[i(l\Delta\omega)(p\Delta t)],\ p = 0, 1, \ldots, M - 1 \tag{46d}$$

$$g_{32}^{(i)}(p\Delta t) = \sum_{l=0}^{M-1} B_{32l}\cdot\exp[i(l\Delta\omega)(p\Delta t)],\ p = 0, 1, \ldots, M - 1 \tag{46e}$$

$$g_{33}^{(i)}(p\Delta t) = \sum_{l=0}^{M-1} B_{33l}\cdot\exp[i(l\Delta\omega)(p\Delta t)],\ p = 0, 1, \ldots, M - 1 \tag{46f}$$

with

$$B_{11l} = 2\left|H_{11}\left(l\Delta\omega + \frac{\Delta\omega}{3}\right)\right|\sqrt{\Delta\omega}\cdot\exp\left[-i\theta_{11}\left(l\Delta\omega + \frac{\Delta\omega}{3}\right)\right]\cdot\exp[i\phi_{1l}^{(i)}] \tag{47a}$$

$$B_{21l} = 2\left|H_{21}\left(l\Delta\omega + \frac{\Delta\omega}{3}\right)\right|\sqrt{\Delta\omega}\cdot\exp\left[-i\theta_{21}\left(l\Delta\omega + \frac{\Delta\omega}{3}\right)\right]\cdot\exp[i\phi_{1l}^{(i)}] \tag{47b}$$

$$B_{22l} = 2\left|H_{22}\left(l\Delta\omega + \frac{2\Delta\omega}{3}\right)\right|\sqrt{\Delta\omega}\cdot\exp\left[-i\theta_{22}\left(l\Delta\omega + \frac{2\Delta\omega}{3}\right)\right]\cdot\exp[i\phi_{2l}^{(i)}] \tag{47c}$$

$$B_{31l} = 2\left|H_{31}\left(l\Delta\omega + \frac{\Delta\omega}{3}\right)\right|\sqrt{\Delta\omega}\cdot\exp\left[-i\theta_{31}\left(l\Delta\omega + \frac{\Delta\omega}{3}\right)\right]\cdot\exp[i\phi_{1l}^{(i)}] \tag{47d}$$

$$B_{32l} = 2\left|H_{32}\left(l\Delta\omega + \frac{2\Delta\omega}{3}\right)\right|\sqrt{\Delta\omega}\cdot\exp\left[-i\theta_{32}\left(l\Delta\omega + \frac{2\Delta\omega}{3}\right)\right]\cdot\exp[i\phi_{2l}^{(i)}] \tag{47e}$$

$$B_{33l} = 2|H_{33}(l\Delta\omega + \Delta\omega)|\sqrt{\Delta\omega}\cdot\exp[-i\theta_{33}(l\Delta\omega + \Delta\omega)]\cdot\exp[i\phi_{3l}^{(i)}] \tag{47f}$$

In (44), (46), and (47), $\Delta\omega$ is defined as [see also (22)]

$$\Delta\omega = \frac{\omega_u}{N} \tag{48}$$

with ω_u being the upper cutoff frequency beyond which the elements of the cross-spectral density matrix [(3)] may be assumed to be zero for either mathematical or physical reasons. Definitions for the Hs, θs and ϕs appearing in (47) have already been provided in (12), (16), and (27), respectively.

At this point it should be mentioned that the technique of digital complex modulation/demodulation developed for FFT-based spectral analysis [e.g., Elliott and Rao (1982)] is used in (44) and (47) to account for the three different definitions of the frequency shown in (21).

Sample function $f_j^{(i)}(p\Delta t)$, $j = 1, 2, 3$ shown in (44) is periodic with period T_0

$$T_0 = 3\frac{2\pi}{\Delta\omega} \tag{49}$$

Hence, Δt and $\Delta\omega$ are related in the following way:

$$3M\Delta t = T_0 = 3\frac{2\pi}{\Delta\omega} \text{ or } M\Delta t = \frac{2\pi}{\Delta\omega} \tag{50a}$$

$$\Delta t = \frac{2\pi}{M\Delta\omega};\ \Delta t\Delta\omega = \frac{2\pi}{M} \tag{50b,c}$$

With the aid of (50c), (46) can be written as

$$g_{jm}^{(i)}(p\Delta t) = \sum_{l=0}^{M-1} B_{jml}\cdot\exp\left[ilp\frac{2\pi}{M}\right],$$

$$j = 1, 2, 3, m = 1, 2, 3, j \geq m;\ p = 0, 1, \ldots, M - 1 \tag{51}$$

It has been established in (28) that in order to avoid aliasing, the time step Δt has to obey the condition

$$\Delta t \leq \frac{2\pi}{2\omega_u} \tag{52}$$

Combining now (48), (50b) and (52), the following condition is established between N and M:

$$M \geq 2N \tag{53}$$

It is obvious that (52) and (53) are equivalent and therefore the time step Δt calculated by (50b) will automatically satisfy the condition set in (52), as long as the condition set in (53) is satisfied.

Instead of using (27) involving a straightforward summation of cosines for digitally generating sample functions of the simulated stochastic vector process, the FFT technique can be readily applied to (51) [followed by the use of (45) and (44)], resulting in a drastic reduction of computer cost.

Finally, it is pointed out that the following condition must be imposed when using (51):

$$B_{jml} = 0 \text{ for } N \leq l \leq M - 1, j = 1, 2, 3, m = 1, 2, 3, j \geq m \tag{54}$$

to account for the assumption that the elements of the cross-spectral density matrix [(3)] are zero for values of the frequency larger than ω_u.

NUMERICAL EXAMPLES

Stochastic Vector Process Description

An example involving simulation of turbulent wind velocity fluctuations is selected in order to demonstrate the capabilities and efficiency of the proposed algorithm. Specifically, the longitudinal velocity fluctuations at three points along a vertical line are considered to be a trivariate stationary stochastic vector process. The three components of this vector process describing the velocity fluctuations at points 1, 2, and 3 (see Fig. 1) are denoted by $f_1^0(t)$, $f_2^0(t)$, and $f_3^0(t)$, respectively. The mean value of the process is equal to zero [see (1)], while the elements of its cross-spectral density matrix [see (3)] are expressed as

$$S_{jj}^0(\omega) = S_j(\omega),\ j = 1, 2, 3 \tag{55}$$

$$S_{jk}^0(\omega) = \sqrt{S_j(\omega)S_k(\omega)}\gamma_{jk}(\omega),\ j, k = 1, 2, 3, j \neq k \tag{56}$$

where $S_j(\omega)$ = power spectral density function of $f_j^0(t)$; and $\gamma_{jk}(\omega)$ = coherence function between $f_j^0(t)$ and $f_k^0(t)$.

At this juncture, it should be pointed out that the stochastic vector process described by (55) and (56) is nonhomogeneous in space, since the longitudinal velocity fluctuations $f_1^0(t)$, $f_2^0(t)$, and $f_3^0(t)$ have different frequency contents [$S_1(\omega) \neq S_2(\omega) \neq S_3(\omega) \neq S_1(\omega)$].

The following form proposed by Kaimal et al. (1972) is selected to model the (two-sided) power spectral density function of the longitudinal wind velocity fluctuations at different heights:

$$S(z, \omega) = \frac{1}{2}\frac{200}{2\pi}u_*^2\frac{z}{U(z)}\frac{1}{\left[1 + 50\dfrac{\omega z}{2\pi U(z)}\right]^{5/3}} \tag{57}$$

where z = height, in meters; ω = frequency, in rad/s; u_* = shear velocity of the flow, in m/s; and $U(z)$ = mean wind speed at height z, in m/s.

The model suggested by Davenport (1968) is chosen for the coherence function between the velocity fluctuations at two different heights z_1 and z_2

$$\gamma(\Delta z, \omega) = \exp\left[-\frac{\omega}{2\pi}\frac{C_z\Delta z}{\frac{1}{2}[U(z_1) + U(z_2)]}\right] \tag{58}$$

where $U(z_1)$ and $U(z_2)$ = mean wind speeds at heights z_1 and z_2, respectively, $\Delta z = |z_1 - z_2|$, and C_z is a constant that can be set equal to 10 for structural design purposes (Kristensen and Jensen 1979; Simiu and Scanlan 1986).

Assuming now that the mean wind speed at point 1 (z = 35 m, see Fig. 1) is $U(35)$ = 45 m/s and that the surface roughness length is z_0 = 0.001266 m (corresponding shear velocity of the flow u_* = 1.76 m/s), the mean wind speeds at point 2 (z = 40 m) and at point 3 (z = 140 m) are computed using the logarithmic law as $U(40)$ = 45.6 m/s and $U(140)$ = 51.1 m/s [the values $U(35)$ = 45 m/s, z_0 = 0.001266 m, and u_* = 1.76 m/s are taken from Simiu and Scanlan (1986), which also provides insightful comments for the expressions shown in (57) and (58)].

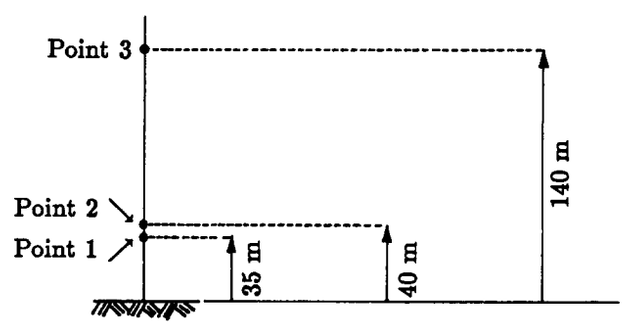

FIG. 1. Configuration of Points 1, 2, and 3 along a Vertical Line

Using the foregoing numerical values, the (two-sided) power spectral density functions of the longitudinal velocity fluctuations [(55)] at points 1, 2, 3 are computed as

$$S_1(\omega) = \frac{38.3}{(1 + 6.19\omega)^{5/3}};\quad S_2(\omega) = \frac{43.3}{(1 + 6.98\omega)^{5/3}};$$

$$S_3(\omega) = \frac{135}{(1 + 21.8\omega)^{5/3}} \tag{59a–c}$$

while the corresponding coherence functions [(56)] are calculated as

$$\gamma_{12}(\omega) = e^{-0.1757\omega},\ \gamma_{13}(\omega) = e^{-3.478\omega},\ \gamma_{23}(\omega) = e^{-3.292\omega} \tag{60}$$

The expressions shown in (59) and (60) are plotted in Figs. 2 and 3, respectively.

Finally, it is straightforward to show [use (57) or refer to Simiu and Scanlan (1986)] that the standard deviation of each of the three components of the vector process is

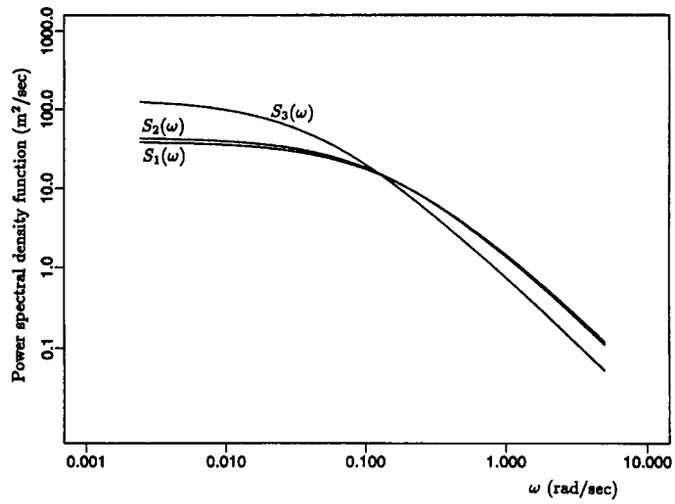

FIG. 2. Power Spectral Density Functions $S_j(\omega)$; j = 1, 2, 3

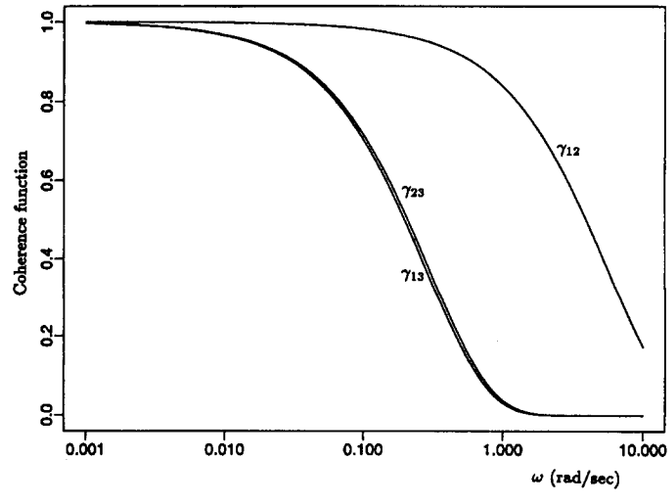

FIG. 3. Coherence Functions $\gamma_{jk}(\omega)$; j, k = 1, 2, 3; $j < k$

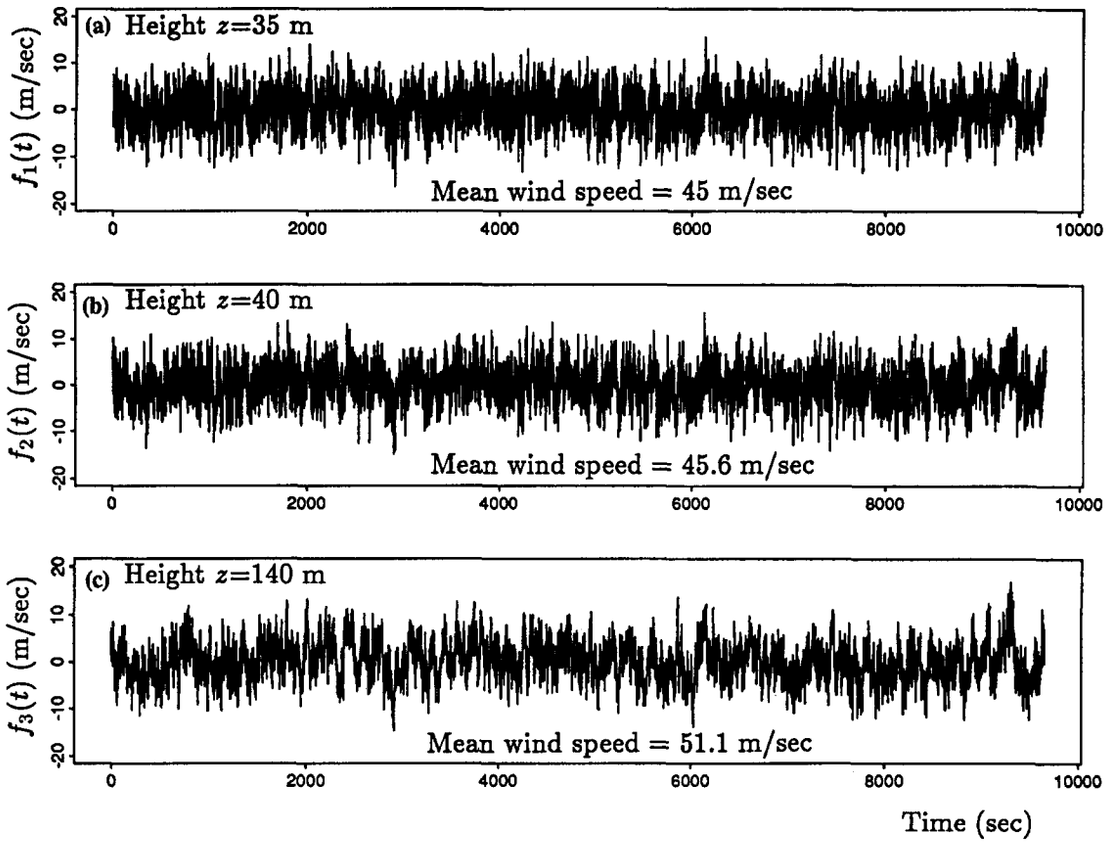

FIG. 4. Generated Sample Function for Longitudinal Wind Velocity Fluctuations at Three Different Heights, over Entire Period T_0 = 9,651 s

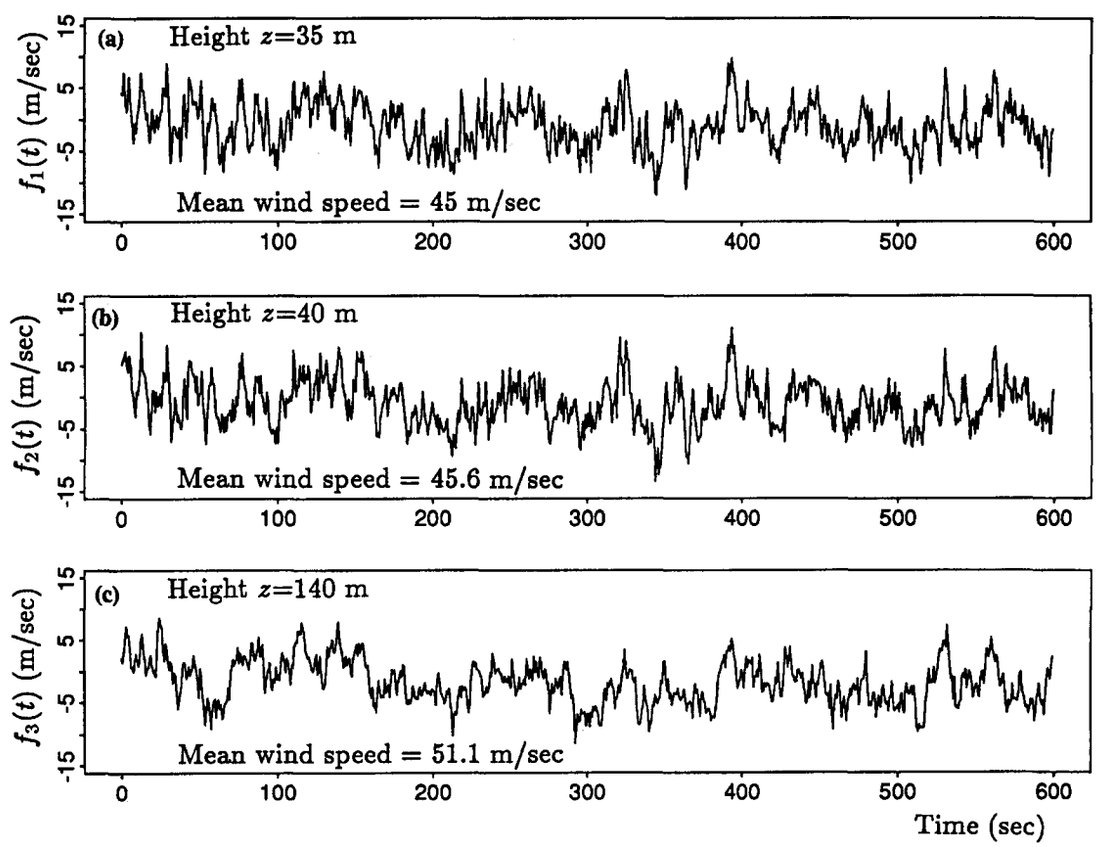

FIG. 5. Generated Sample Function for Longitudinal Wind Velocity Fluctuations at Three Different Heights, over First 600 s of Period T_0 (T_0 = 9,651 s)

J. Eng. Mech. 1996.122:778-787.

$$\sigma = \sqrt{6}u_* = 4.31 \text{ m/s} \quad (61)$$

Simulation of Stochastic Vector Process by FFT

To perform the generation of sample functions of the stochastic vector process according to (44), (45), and (51), which take advantage of the FFT technique, the upper cutoff frequency ω_u [see (22)], the value of N [see (22)], and the value of M [see (44)] are set equal to

$$\omega_u = 4.0 \text{ rad/s}; \quad N = 2{,}048; \quad M = 4{,}096 = 2^{12} \quad (62a\text{–}c)$$

Then, $\Delta\omega$, Δt, and T_0 are calculated using (22), (50*b*), and (49) as

$$\Delta\omega = 0.00195 \text{ rad/s}; \quad \Delta t = 0.785 \text{ s}; \quad T_0 = 9{,}651 \text{ s} \quad (63a\text{–}c)$$

Finally, the condition set on the time step Δt by (52) is satisfied, since the equivalent condition set in (53) on M and N is satisfied.

Before proceeding with the generation of sample functions of the stochastic vector process $f_j^0(t)$, $j = 1, 2, 3$, the upper bound for $f_j^{(i)}(t)$, $j = 1, 2, 3$ given by (29) is calculated using $N = 128$ as

$$f_1^{(i)}(t) \leq 49.1 \text{ m/s}; f_2^{(i)}(t) \leq 63.7 \text{ m/s}; f_3^{(i)}(t) \leq 49.2 \text{ m/s} \quad (64a\text{–}c)$$

Considering that the standard deviation of the process is 4.31 m/s [see (61)], it is obvious that the upper bounds shown in (64) are large enough for all practical applications.

A sample function $f_j^{(i)}(t)$, $j = 1, 2, 3$ of the stochastic vector process is now generated using (44), (45), and (51), which take advantage of the FFT technique. As mentioned, the generation is performed at $3 \cdot M = 3 \cdot 4{,}096 = 12{,}288$ time instants, with a time step $\Delta t = 0.785$ s [see (63)], over a length equal to one period $T_0 = 9{,}651$ s [see (63)]. The generated sample function for the longitudinal wind velocity fluctuations at points 1, 2, and 3 (see Fig. 1), denoted by $f_1(t)$, $f_2(t)$, and $f_3(t)$, respectively, is displayed in Fig. 4 for the entire period $T_0 = 9{,}651$ sec and in Fig. 5 for the first 600 sec in order to better visualize the differences and the similarities among the three time histories.

The different frequency contents of $f_1(t)$, $f_2(t)$, and $f_3(t)$ (making the wind velocity fluctuations nonhomogeneous in space) can be detected in Fig. 5. Specifically, $f_1(t)$ and $f_2(t)$ have very similar frequency contents, while $f_3(t)$ has a relatively lower one, as indicated by their respective power spectral density functions displayed in Fig. 2. As far as the degree of correlation among the three time histories is concerned, it is clearly seen in Fig. 5 that since points 1 and 2 are only 5 m apart, there is only a small loss of coherence between $f_1(t)$ and $f_2(t)$. On the other hand, there is a considerable loss of coherence between $f_1(t)$ and $f_3(t)$ [and between $f_2(t)$ and $f_3(t)$], as point 3 is located 105 m from point 1 and 100 m from point 2 (see Fig. 1). This behavior is controlled by the coherence functions plotted in Fig. 3.

It is therefore obvious from Fig. 5 that the proposed algorithm is able to simulate longitudinal wind velocity fluctuations that are spatially correlated according to a prescribed coherence function, and are nonhomogeneous in space (or equivalently they have different frequency contents).

The temporal auto-/cross-correlation function $R_{jk}^{(i)}(\tau)$, $j, k = 1, 2, 3$ of the generated sample function shown in Fig. 4 is computed and plotted versus the target auto-/cross-correlation function $R_{jk}^0(\tau)$, $j, k = 1, 2, 3$ in Fig. 6 [note that $R_{jk}^0(\tau)$, $j, k = 1, 2, 3$ is computed numerically using (7)]. As seen in Fig. 6, $R_{jk}^{(i)}(\tau)$ practically coincides with $R_{jk}^0(\tau)$, $j, k = 1, 2, 3$, thus confirming the conclusion drawn in the section titled "Ergo-

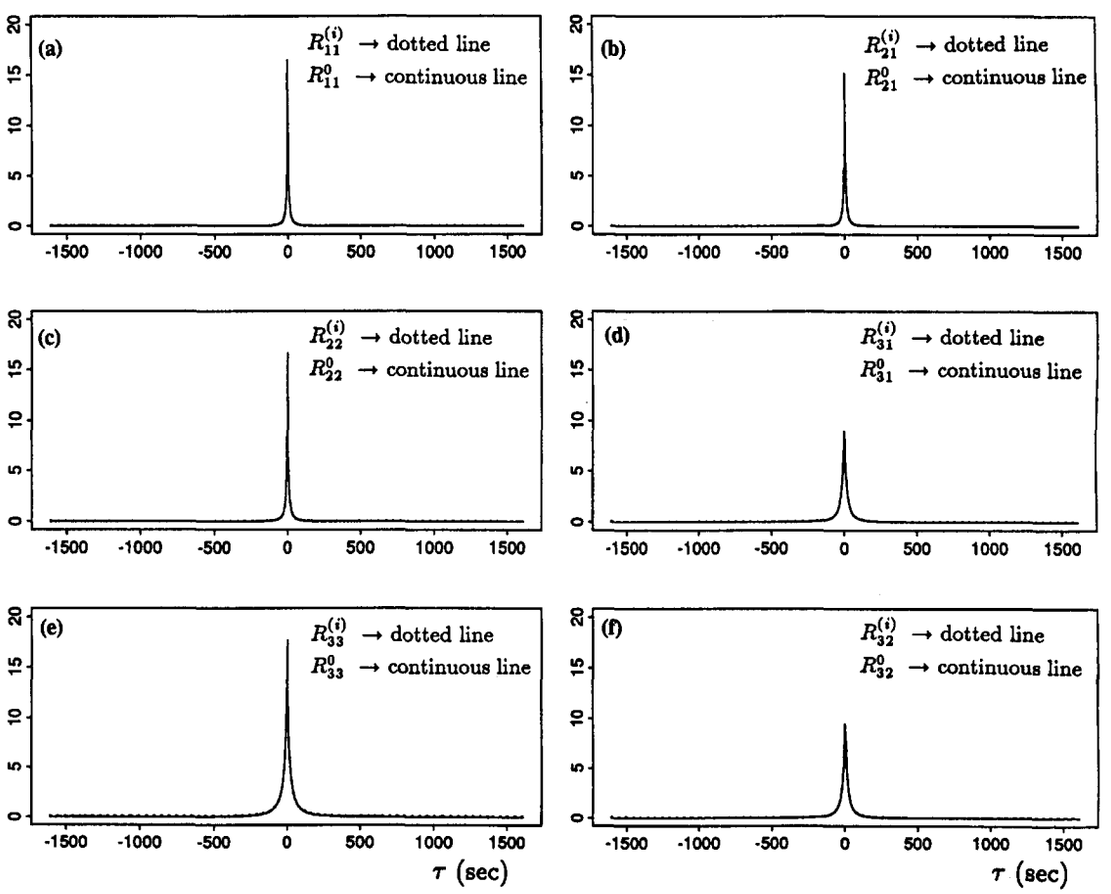

FIG. 6. Temporal Auto-/Cross-Correlation Functions [$R_{jk}^{(i)}(\tau)$] of Generated Sample Function Displayed in Fig. 4 versus Corresponding Targets [$R_{jk}^0(\tau)$]

J. Eng. Mech. 1996.122:778-787.

dicity of Simulated Stochastic Vector Process" that the temporal auto-/cross-correlation function of any sample function $f_j^{(i)}(t), j = 1, 2, 3$ is identical to the target auto-/cross-correlation function when the length of the sample function is equal to the period T_0. At this juncture, if the temporal auto-/cross-correlation function is computed using only part of the period T_0 of the generated sample function, it will not coincide with the corresponding target auto-/cross-correlation function. In such a case, only the ensemble auto-/cross-correlation function will coincide with the corresponding target auto-/cross-correlation function. However, this does not constitute a serious limitation to the ergodicity property of the proposed algorithm, since the period T_0 of the generated sample functions is directly controlled (and can become arbitrarily large) by parameter N [see (26) and (22)].

Finally, the generation of the three time histories shown in Fig. 4 (each one at 12,288 time instants) requires only 2 MB of memory (for double precision computations) and takes 4 s of central processing unit (CPU) time on a Silicon Graphics Indigo2 computer.

CONCLUSIONS

A simulation algorithm was proposed to generate sample functions of a stationary, multivariate stochastic process according to its prescribed cross-spectral density matrix. If the components of the vector process correspond to different locations in space, the process is nonhomogeneous in space. The proposed algorithm generates ergodic sample functions in the sense that the temporal cross-correlation matrix of each and every generated sample function is identical to the corresponding target, when the length of the sample function is equal to one period. The algorithm is very efficient computationally since it takes advantage of the fast Fourier transform technique.

An example involving simulation of turbulent wind velocity fluctuations was presented in order to demonstrate the capabilities and efficiency of the proposed algorithm. Specifically, the longitudinal velocity fluctuations at three points along a vertical line were considered to be a trivariate, stationary stochastic vector process. The generated wind velocity time histories were spatially correlated according to a given coherence function and were nonhomogeneous in space (or equivalently they had different prescribed frequency contents).

Finally, the proposed algorithm has several other applications. Two representative ones are the following: simulation of different correlated material properties along the length of a one-dimensional structure (e.g., for a beam: mass density, viscous damping, and flexural stiffness), and simulation of correlated seismic ground motion time histories at different locations on the ground surface. Referring to the latter application, it should be mentioned that using the proposed algorithm, acceleration, velocity, or displacement time histories can be generated at several locations on the ground surface according to a prescribed cross-spectral density matrix (specifically, a different prescribed power spectrum at each location, a prescribed coherence function, and a prescribed velocity of wave propagation). Another advantage of the proposed simulation algorithm is that, due to its ergodicity property, the temporal cross-spectral density matrix of every sample function of the ground motion time histories will be identical to the prescribed target cross-spectral density matrix (this is the case when the length of the sample function is equal to one period, as mentioned earlier in this paper). Consequently, it is not necessary to generate a large number of sample functions in order to accurately reproduce the target cross-spectral density matrix through an ensemble average. This can result in substantial computational savings. At this juncture, it should be reminded that although the assumption of stationarity is frequently used in earthquake engineering with good results, seismic ground motion is inherently nonstationary. For this reason, as part of future work, the proposed algorithm will be modified to simulate nonstationary vector processes with evolutionary power.

ACKNOWLEDGMENTS

This work was supported by the National Science Foundation under Grant No. BCS-9257900 with Clifford J. Astill as program director, and by the NCEER Highway Project (FHWA Contract DTFH61-92-C-00106).

APPENDIX. REFERENCES

Bracewell, R. N. (1986). *The Fourier transform and its applications*. McGraw-Hill Book Co., Inc., New York, N.Y.

Brigham, E. O. (1988). *The fast Fourier transform and its applications*. Prentice-Hall, Inc., Englewood Cliffs, N.J.

Davenport, A. G. (1968). "The dependence of wind load upon meteorological parameters." *Proc., Int. Res. Seminar on Wind Effects on Build. and Struct.*, University of Toronto Press, Toronto, Canada, 19–82.

Deodatis, G. (1996). "Simulation of stochastic processes and fields to model loading and material uncertainties." *Probabilistic methods for structural design*, C. G. Soares, ed., Kluwer Academic Publishers, Boston, Mass.

Deodatis, G., and Shinozuka, M. (1989). "Simulation of seismic ground motion using stochastic waves." *J. Engrg. Mech.*, ASCE, 115(12), 2723–2737.

Elishakoff, I. (1983). *Probabilistic methods in the theory of structures*. John Wiley & Sons, Inc., New York, N.Y.

Elliott, D. F., and Rao, K. R. (1982). *Fast transforms: algorithms, analyses, applications*. Academic Press, Inc., New York, N.Y.

Gersch, W., and Yonemoto, J. (1977). "Synthesis of multi-variate random vibration systems: a two-stage least squares ARMA model approach." *J. Sound and Vibration*, 52(4), 553–565.

Grigoriu, M. (1993). "On the spectral representation method in simulation." *J. Probabilistic Engrg. Mech.*, 8(2), 75–90.

Grigoriu, M. (1995). *Applied non-Gaussian processes*. Prentice-Hall, Inc.

Kaimal, J. C. et al. (1972). "Spectral characteristics of surface-layer turbulence." *J. Royal Meteorological Soc.*, London, England, 98, 563–589.

Kareem, A., and Li, Y. (1991). "Simulation of multi-variate stationary and non-stationary random processes: a recent development." *Proc., 1st Int. Conf. on Computational Stochastic Mech.*, Elsevier Applied Science, New York, N.Y., 533–544.

Kozin, F. (1988). "Auto-regressive moving-average models of earthquake records." *J. Probabilistic Engrg. Mech.*, 3(2), 58–63.

Kristensen, L., and Jensen, N. O. (1979). "Lateral coherence in isotropic turbulence and in the natural wind." *Boundary Layer Meteorology*, 17, 353–373.

Li, Y., and Kareem, A. (1993). "Simulation of multi-variate random processes: hybrid DFT and digital filtering approach." *J. Engrg. Mech.*, ASCE, 119(5), 1078–1098.

Mignolet, M. P., and Spanos, P.-T.D. (1987a). "Recursive simulation of stationary multi-variate random processes. Part I." *J. Appl. Mech.*, 54(3), 674–680.

Mignolet, M. P., and Spanos, P.-T.D. (1987b). "Recursive simulation of stationary multi-variate random processes. Part II." *J. Appl. Mech.*, 54(3), 681–687.

Ramadan, O., and Novak, M. (1993). "Simulation of spatially incoherent random ground motions." *J. Engrg. Mech.*, ASCE, 119(5), 997–1016.

Rice, S. O. (1954). "Mathematical analysis of random noise." *Selected papers on noise and stochastic processes*, N. Wax, ed., Dover Publ. Inc., New York, N.Y., 133–294.

Shinozuka, M. (1972). "Monte Carlo solution of structural dynamics." *Comp. and Struct.*, 2(5+6), 855–874.

Shinozuka, M. (1974). "Digital simulation of random processes in engineering mechanics with the aid of FFT technique." *Stochastic problems in mechanics*, S. T. Ariaratnam and H. H. E. Leipholz, eds., Univ. of Waterloo Press, Waterloo, Canada, 277–286.

Shinozuka, M. (1987). "Stochastic fields and their digital simulation." *Stochastic methods in structural dynamics*, G. I. Schuëller and M. Shinozuka, eds., Martinus Nijhoff Publishers, Dordrecht, The Netherlands, 93–133.

Shinozuka, M., and Deodatis, G. (1988). "Stochastic process models for earthquake ground motion." *J. Probabilistic Engrg. Mech.*, 3(3), 114–123.

Shinozuka, M., and Deodatis, G. (1991). "Simulation of stochastic processes by spectral representation." *Appl. Mech., Rev.*, 44(4), 191–204.

Shinozuka, M., and Jan, C.-M. (1972). "Digital simulation of random processes and its applications." *J. Sound and Vibration*, 25(1), 111–128.
Shinozuka, M., Kamata, M., and Yun, C.-B. (1989). "Simulation of earthquake ground motion as multi-variate stochastic process." *Tech. Rep. No. 1989.5*, Princeton-Kajima Joint Res., Dept. of Civ. Engrg. and Operations Res., Princeton University, Princeton, N.J.
Simiu, E., and Scanlan, R. H. (1986). *Wind effects on structures*. John Wiley & Sons, Inc., New York, N.Y.
Soong, T. T., and Grigoriu, M. (1993). *Random vibration of mechanical and structural systems*. Prentice-Hall, Inc., Englewood Cliffs, N.J.
Yamazaki, F., and Shinozuka, M. (1988). "Digital generation of non-Gaussian stochastic fields." *J. Engrg. Mech.*, ASCE, 114(7), 1183–1197.
Yang, J.-N. (1972). "Simulation of random envelope proceses." *J. Sound and Vibration*, 25(1), 73–85.
Yang, J.-N. (1973). "On the normality and accuracy of simulated random processes." *J. Sound and Vibration*, 26(3), 417–428.

J. Eng. Mech. 1996.122:778-787.